

Submitted to ApJ, 1999, September 27th

## The timing evolution of 4U 1630-47 during its 1998 outburst

S.W. Dieters<sup>1,8</sup>, T. Belloni<sup>2</sup>, E. Kuulkers<sup>3</sup>, P. Woods<sup>1,8</sup>, W. Cui<sup>4</sup>, S.N. Zhang<sup>1</sup>, W. Chen<sup>5</sup>, M. van der Klis<sup>6</sup>, J. van Paradijs<sup>1,6</sup>, J. Swank<sup>5</sup>, W.H.G Lewin<sup>4</sup>, C. Kouveliotou<sup>7,8</sup>

### ABSTRACT

We report on the evolution of the timing of 4U 1630-47 during its 1998 outburst using data obtained with the Rossi X-ray Timing Explorer (RXTE). The count rate and position in hardness-intensity, color-color diagrams and simple spectral fits are used to track the concurrent spectral changes. The source showed seven distinct types of timing behavior, most of which show differences with the canonical black hole spectral/timing states. In marked contrast to previous outbursts, we find quasi-periodic oscillation (QPO) signals during nearly all stages of the outburst with frequencies between 0.06 Hz and 14 Hz and a remarkable variety of other characteristics. In particular we find large (up to 23% rms) amplitude QPO on the early rise. Later, slow 0.1 Hz semi-regular short ( $\sim 5$  sec), 9 to 16% deep dips dominate the light curve. At this time there are two QPOs, one stable near 13.5 Hz and the other whose frequency drops from 6–8 Hz to  $\sim 4.5$  Hz during the dips. BeppoSAX observations during the very late declining phase show 4U 1630-47 in a low state.

*Subject headings:* accretion, accretion disks —, binaries: close — X-rays: stars — stars: individual 4U 1640-47

---

<sup>1</sup>University of Alabama in Huntsville, 301 Sparkman Dr., Huntsville, AL 35899, USA.

<sup>2</sup>Osservatorio Astronomico di Brera, Via E. Bianchi 46, I-23807, Merate (LC), Italy

<sup>3</sup>Space Research Organization Netherlands, Sorbonnelaan 2, 3584 CA, Utrecht, The Netherlands, & Astronomical Institute, Utrecht University

<sup>4</sup>Massachusetts Institute of Technology, Center for Space Research, Cambridge, MA 02139, USA

<sup>5</sup>NASA/Goddard Space Flight Center, Code 661, Greenbelt, MD 20771, USA

<sup>6</sup>Astronomical Institute “Anton Pannekoek”, University of Amsterdam, Kruislaan 403, 1098 SJ Amsterdam, The Netherlands

<sup>7</sup>Universities Space Research Association

<sup>8</sup>NASA/Marshall Space Flight Center, SD-50, Huntsville, AL 35812

## 1. INTRODUCTION

4U 1630-47 has shown recurrent X-ray outbursts with intervals of 600–700 days (Jones et al. 1976, Friedhorsky 1986, Kuulkers et al. 1997a). This is much shorter than the typical waiting time of 10–50 yrs for soft X-ray transients (Tanaka & Lewin 1995), which makes 4U 1630-47 an important source for studying how the spectral/timing behavior depends upon mass accretion rate and/or other parameters.

4U 1630-47 is a black-hole candidate (Parmar, Stella & White 1986, Barret, McClintock & Grindlay 1996, Kuulkers et al. 1997a) because it has shown spectral and timing characteristics similar to those of other X-ray sources with a measured high mass function. The X-ray emission of black hole candidates (BHCs) is usually classified into four timing/spectral states, which are in order of increasing X-ray flux and presumably mass accretion rate: low, intermediate, high and very high states (see van der Klis 1995; Cui 1999). In the Low State (LS) the power density spectrum (PDS) shows strong (30–50% rms) band-limited (flat-topped) noise with a break between 0.03 and 0.3 Hz and the energy spectrum is well fit with a power law with index of  $\Gamma = -1.5$ – $-2.5$  up to at least 200 keV (Gilfanov et al. 1994). In the High State (HS) the PDS shows weak (few % rms) power law noise. The energy spectrum is dominated by a soft component which can be satisfactorily fit by a multi-temperature disk blackbody. The fitted temperature ( $kT \sim 1$  keV) and innermost radius are comparable to values expected for a stellar mass black hole. In the very high state (VHS) the soft component increases in flux by a further factor 2–8 over that in the high state. The power law component strengthens and is visible in the energy spectra. The power density spectrum shows a variable broad band component and 3–10 Hz QPO. The noise component is either band-limited with a break between 1 and 20 Hz, or a power law similar to that in the high state. Occasionally at times between a HS and a LS an intermediate state (IS) is observed e.g. GX 339-4 (Méndez & van der Klis 1997), GS 1124-68 (Belloni et al. 1997a), GRO J1655-40 (Méndez, Belloni & van der Klis 1998) and Cyg X-1 (Belloni et al. 1996, Cui et al. 1997). The intermediate state has fluxes and spectral properties intermediate those of the HS and LS (Rutledge et al. 1999). The power spectral properties are very much like the VHS. Slow  $< 1$  Hz QPO have been observed in all states.

4U 1630-47 has quite variable outbursts. The 1996 outburst, lasted  $\sim 50$  days, the 1977 outburst lasted  $\sim 10$  months and the 1988–91 interval showed ongoing long term activity (Kuulkers et al. 1997b). Even though the 1987 and 1996 outbursts had similar flux histories they show opposite trends in spectral hardness as a function of time (Kuulkers et al. 1997a). Such a range in behavior is akin to the variety of outbursts of the superluminal jet sources GRS 1915+105 and GRO 1655-40.

There are other similarities between 4U 1630-47 and these sources. During the 1998 outburst radio emission was detected just as the source was making a transition from hard to soft emission (Hjellming et al. 1999). This is very similar to the behavior of GRS 1739-278 and jet sources. Also 4U 1630-47 showed strong linear polarization in its radio flux, which has only been observed

in elongated jet sources like SS433, GRS 1915+105 and GRO 1655-40 (Hjellming et al. 1999 and references therein).

Absorption dips lasting 50–150 sec and reaching 8–30% of the non-dip flux have been observed from 4U 1630-47 (Kuulkers et al. 1997b, Tomsick, Lapshov & Kaaret 1998). These dips, indicate that like GRO 1655-40 and the accretion disk corona sources, 4U 1630-47 is being viewed at a high (60–75°) inclination. This cannot be confirmed since no optical counterpart has so far been identified (Parmar et al. 1986, Buxton, private communication). Also it is expected that these absorption dips will occur over a restricted range in phase and so yield an estimate of the orbital period. We find no evidence for any absorption dips in our data.

The 1998 outburst began with a slow rise in the 20–100 keV (BATSE) flux starting near January 28 (TJD 10841; TJD=JD-2,440,000.5). Later on February 3 (TJD 10847) the RXTE all sky monitor (ASM; Levine et al. 1996) began showing 2–12 keV flux. Radio emission is thought to have started just as soft flux began its rapid rise near February 7 (TJD 10851). RXTE PCA observations were triggered at this time. This outburst was well covered (100 observations) by RXTE (this paper, Tomsick & Kaaret 1999), ROSAT HRI/PSPC (between February 17 and 28), BeppoSAX (Oosterbroek et al. 1998), ASCA (February 25–26) and BATSE and radio (Hjellming et al. 1999). In this paper we discuss the evolution of the timing behavior during the 1998 outburst.

Between May and September 1999, well in advance of its next expected outburst (mid-December 1999; Kuulkers et al. 1998) 4U 1630-47 underwent a fainter than normal outburst. In terms of the very early flux evolution in the BATSE and RXTE ASM energy ranges, the 1999 outburst was almost identical to that in 1998. On the very early rise (1999 May 8) a single 0.85 Hz, 16% rms QPO peak was found in the power density spectrum (McCullough et al. 1999). At this time the energy spectrum was hard. An observation two days later failed to find any QPO.

## 2. OBSERVATIONS

The observations discussed here (Obs. ID: 30178-0[1-2]- and 30188-02-) were taken with the RXTE PCA (Jahoda et al. 1996) roughly daily, beginning on 1998 February 9, till 4U 1630-47 reached maximum on February 22. After maximum our observations were made every 2–5 days till 1998 March 31. Observations that partially overlap ours and extend until 1998 June 8 are reported by Tomsick & Kaaret (1999).

We analyzed 49 observations, most of which are  $\sim 1.4$  ksec in length. For each of the pointings we calculated power density spectra from segments of data 1, 2, 16, 256 seconds long, using the whole energy range 2–60 keV. The time resolution is mostly 2 ms. Power spectra were selected by time and intensity so that the resulting average spectra are representative of the different flux levels within each observation. In many observations the count rate did not vary much and one average power density spectrum was sufficient to characterize the observation. The averaged power density spectra were normalized to the rms variability (Belloni & Hasinger 1990) using the

average background as estimated using the PCABACKEST V2.1b, and corrected for dead-time (Zhang et al. 1995, Zhang 1995).

The average count rate, two hardness ratio's, and PHA spectra were determined for each observation using Standard 2 mode data from only a single PCA detector (PCU 0). Data selection and background subtraction followed standard procedures.

In addition we present two serendipitous BeppoSAX observations made with the MECS (Boella et al. 1997) on 1998 August 7 (TJD 11032) and 1998 September 16 (TJD 11072). SAX was pointed at SGR 1621-47, placing 4U 1630-47 at the edge of the field of view with an offset of 22'. The on source times were 85.7 and 62.4 ksec, respectively. Source counts were collected from a 30' diameter circle that included the entire elongated image of 4U 1630-47. Background counts were extracted from a circular patch of the same size centered at the same offset on the opposite side of the MECS field of view. The response matrix was that for a 20' offset. The expected resulting systematic errors on the spectrum are 5–10%.

### 3. RESULTS

During the outburst, seven distinct types of timing behavior occurred. We label the different behaviors as A,B(b),C,D,E,F,G. The distinctions are primarily in the shape of the broad band noise, and secondarily in the properties of the QPO. The timing properties change hand-in-hand with changes in the energy spectrum. Figure 1 gives an overview of the count rate and spectral changes as represented by two lightcurves, a hardness-intensity and a color-color diagram. Figure 2 shows from our data, five representative power density spectra (behaviors A,B,C,D,E), whose fit parameters are given in Table 1.

#### 3.1. Timing properties

**A** During the first RXTE observation (1998 February 9, TJD 10854) while 4U 1630-47 was in the initial stages of its rise to maximum, a pair of very strong (25% and 5.6% rms) QPOs were discovered in the power density spectrum (Dieters et al. 1998a) at frequencies of 2.67 and 5.62 Hz respectively. These are the first QPOs found from this source (except the marginal detection of Kuulkers et al. 1998) and they are amongst the largest amplitude QPOs ever measured from a BHC (see Fig. 2, panel A). Similar large amplitude QPO were observed in the second observation. The power density spectra were fit with 3 Lorentzians to describe the peaks and a broken (flat topped) power law to describe the broad-band noise. The lower frequency peak was asymmetric with a shoulder toward higher frequencies. A Lorentzian was used to fit this shoulder. The central frequencies of the two QPOs are not formally consistent with the peaks being harmonically related but the frequencies are commensurate to well within the widths of the QPO peaks. The quality factor  $Q$  (ratio of frequency to FWHM), is 12 and 8 in the 1st and 2nd observations for the

lower frequency QPOs and 3–5 for the shoulder and upper frequency QPO. Between the first two observations the count rate increased by a factor of 1.26, the QPO frequencies increased (lower QPO: 2.67 to 3.20 Hz, upper QPO: 5.62 to 6.66 Hz), the amplitude of the QPOs decreased (lower QPO: 17.03 to 15.29% rms, upper QPO 5.79 to 4.16% rms), the amplitude of the broad band noise remained roughly constant at 20% rms, and the break frequency increased from  $0.67 \pm 0.03$  Hz to  $0.94 \pm 0.06$  Hz.

**B** After the first two observations, there was a 1 day gap in RXTE observations, during which 4U 1630-47 brightened rapidly (Fig. 1). Between TJD 10856 and TJD 10864, 4U 1640-47 continued to brighten, but at an ever decreasing rate, forming a “shoulder” in the overall light curve. Short, sharp dips appeared. These dips were generally triangular in shape with a sharp drop ( $\leq 1$  sec) followed by a rise lasting 3–5 sec. Initially they were weak and fairly sporadic, but as the count rate increased they became more regular, more closely spaced and deeper (9–16%), dominating the light curve (Fig. 3). Toward the end of the shoulder the depth and the frequency of these dips started to decrease. In the power density spectrum these dips show up as a QPO peak near 0.1 Hz and occasionally its harmonic (See Fig. 2, panel B). The underlying power density spectrum is again modeled as a broken power law but the power density spectrum below the break (generally at 0.1–0.8 Hz) is not flat (index mostly 0.1–0.5). The noise amplitude is much weaker (4.6–9.7% rms) than in the initial (A) observations. Three peaks are observed in the power density spectra, typically at: 3–5 Hz (increasing with count rate), 6–8 Hz (no long term trend with count rate), and near 13.5 Hz (roughly constant), with rms amplitudes of 7–4%, 4–1%,  $\sim 2\%$ , respectively. The amplitudes generally decreased with count rate and time. The QPO near 13.5 Hz is weak and can only be detected in our longer observations. Because of the gap in observations, we cannot tell if these three QPO are the same as those seen in A. The highest frequency QPO has  $Q \sim 9$ . The  $Q$  of the lower two peaks (2–7) is lower than the QPOs of A. This is especially true for the lowest frequency peak.

We find two observations (denoted as b in Fig. 1) outside the shoulder in which dipping behavior reappears; one near maximum (C) and the other on the decline (D). In both cases the count rates and colors (spectra) become comparable to those in the plateau. Within the Tomsick & Kaaret data set there are two further instances where dipping reappears on the decline. These observations were made on the two days preceding our observation.

We investigated the behavior of the QPOs in and outside the dips using 1 and 2 second data segments sorted by count rate. We found that the  $\sim 13.5$  Hz QPO remained constant in amplitude and frequency. However, the QPO peak with a frequency near 6–8 Hz, dropped in frequency to  $\sim 4.5$  Hz within the dips while remaining at a similar amplitude. There are only 2 QPOs: one stable near 13.5 Hz, the other moving from 6–8 Hz outside the dips to 4–5 Hz. This explains the 3 peaks in Fig. 2B at 13.6, 7, and 5 Hz. The width of the QPO peaks is larger than just that expected from the QPO being truncated on entering and leaving the dips. This is consistent with either the frequency varying, or the wave-trains that make up the lower frequency QPO being in general shorter than the dips, i.e.  $< 5$  seconds.

**C** On about 1998 February 18, (TJD 10863, Fig 1), the ASM/PCA count rate increases rapidly reaching a broad roughly constant maximum until February 24 (TJD 10869), after which the count rate drops rapidly. Here there are no dips and the power density spectrum shows weak (0.5–2.3%), broad (few Hz) QPO with frequencies in the 6.5–9.5 Hz range superimposed upon a power law (slope 1.0–1.9) continuum (1.4–2.7% rms.), see Fig. 2C. Occasionally, an extra (< 2% rms) Lorentzian component peaking in the 1–2 Hz was required in the fits. This peak is similar to the marginal QPO detection of Kuulkers et al. (1998).

**D** After the sharp drop ( $\leq 1$  day) on TJD 10869, the flux continues to decline with count rates ranging from those of B to A. The power density spectrum shows a broad bump near 1 Hz, there is a steep component at very low ( $< 0.1$  Hz) frequencies and a 2% rms amplitude QPO peak near 11 Hz. Note that this steep component is similar in amplitude and slope to the power law component of C. The broad band noise was modeled with either a flat-topped power law with a break near 1 Hz and a zero-frequency Lorentzian or by a power law and a broad Lorentzian peak near 1 Hz (see Fig. 2D). The broad bump contributed 2.4–4.4% rms, generally increasing as flux declined. The very low frequency component became generally weaker (max 1.8% rms.) as 4U 1630-47 faded. This sort of power density spectrum persisted even as the count rate dropped to levels where large amplitude QPO (A) were observed on the rise. The colors in these decline observations are different from those of the same flux on the rise.

**E** In the last two observations beyond TJD 10850 the very low frequency component disappears and the power density spectrum can be well fit by just a flat-topped broken power law. The change from D to E seems to be gradual and continuous. The break frequency is near 1 Hz, the slope above the break  $\sim 1.5$ , and the amplitude  $\sim 3\%$  rms. This flat-topped noise is very similar to the  $\sim 1$  Hz bump seen on the decline (D) and could well be the same component. The absorbed flux (2–10 keV) in our last observation (TJD 10873) is  $1.9 \times 10^{-9} \text{ erg cm}^{-2} \text{ s}^{-1}$ .

**F** Much later (at TJD 10950), Tomsick & Kaaret (1999) report a marked change in the power density spectra; from spectra with  $\leq 4\%$  rms noise (like E) to spectra with  $> 10\%$  rms broad band noise and a single 3.38 Hz, QPO with 19% rms amplitude. The QPO frequency decreased to about 0.2 Hz as 4U 1630-47 faded to a absorbed flux (2–10 keV) of  $\sim 3 \times 10^{-10} \text{ erg cm}^{-2} \text{ s}^{-1}$  at TJD 10972 (their last observation, and last scheduled for RXTE).

Eighteen days later (1998 June 26, TJD 10990) during an RXTE PCA observation of SGR 1627-41 which included 4U 1630-47 within the field of view (FOV; response 37%) 0.15 Hz QPO were found (Dieters et al. 1998b). The amplitude was at least 3% rms. The actual amplitude is dependent upon the relative contributions to the flux from SGR 1627-41, 4U 1630-47 and the local galactic ridge emission. Given that BeppoSAX observations made on the 1998 August 7 (TJD 11032) and 1998 September 16 (TJD 11072) show that 4U 1630-47 was still much brighter than SGR 1627-41, and that SGR 1627-41 was in quiescence and hence fainter (Woods et al. 1999) while Tomsick & Kaaret (1999) found 3.4–0.2 Hz QPO, it is reasonable to suppose that the 0.15 Hz QPO originate from 4U 1630-47. Thus the amplitude of the 0.15 Hz QPO must be at least

8.2% rms.

### 3.2. Spectral evolution

For each observation, the energy spectrum is modeled with the combination of a multi-color disk component and a power-law component, which is typical for black hole candidates (Tanaka & Lewin 1995). Such parameterization can adequately describe the observed X-ray spectrum of 4U 1630-47, although an additional Gaussian component is always required, probably indicating the presence of an iron  $K_\alpha$  line. Significant residuals still remain in some cases (especially C and D), but the results are good enough to provide a rough description of the spectral evolution of the source during the outburst. More detailed spectral results and discussions will be presented elsewhere (Cui, Zhang, Sun et al. 1999, in preparation). The decline is also partially covered by BeppoSAX observations (Oosterbroek et al. 1998; their observations 1.1–1.5 occur when we find 4U 1630-47 in behaviors to C, C, D or possibly b, D, E respectively).

Following the onset of the outburst (the first four observations, covering A and the transition into B), both the soft component and the power-law component strengthen. Initially (A) the soft component is the weaker, contributing  $\lesssim 20\%$  of the total (1.5–60 keV) flux. At the same time, the power law steepens (the photon index goes from  $-2.0$  to  $-2.5$ ) as shown by the changes in the color-color diagram of Fig. 1. This is consistent with the results from simultaneous ASM and BATSE observations (Hjellming et al. 1999). During B, the two components both grow in strength with each contributing about half the unabsorbed flux.

Moving to C, the absorption increases ( $9-10$  as opposed to  $8-8.5 \times 10^{22}$  atoms  $\text{cm}^{-2}$ ) the power law component becomes stronger ( $\sim 60\%$ ) relative to the soft (disk) component. As C progresses, the power law component weakens and becomes steeper (photon index reaches as steep as  $-2.8$ ). The combination of higher absorption and steepening power law move 4U 1630-47 away from the pure-power laws toward the pure blackbody curves on the color-color diagram (Fig. 1).

The decaying period (D and E), begins with the soft component contributing most of the flux ( $60-70\%$ ) at a somewhat lower temperature ( $kT=1.2$  keV rather than  $1.4-1.5$  of C). As the count rate drops, the absorption also drops, the soft component weakens and becomes softer while the power law component flattens. In E the soft component contributes at most  $45-55\%$  of the flux, the absorption is ( $4-7 \times 10^{22}$  atoms  $\text{cm}^{-2}$ ) and the power law index is  $\sim -2$ . This combination of changes move 4U 1630-47 to the right and lower on the color-color diagram (Fig. 1). These trends continue in F, with the soft component contributes at most  $10\%$  of the  $2-60$  keV flux, the power law index being in the range  $-1.4$  to  $-1.8$  and the absorption a little lower still. Thus the energy spectra indicate a further hardening of the source i.e. more like A.

### 3.3. The BeppoSAX data

**G** The BeppoSax MECS(2&3) PHA spectra can be adequately fit (August: reduced  $\chi^2 = 0.8757$  with 92 dof, September: reduced  $\chi^2 = 1.5168$  with 92 dof) with a simple absorbed power-law model. We used 3 and 4 channel re-binning over the 1.8 to 11.5 keV range. The best fit parameters for 1998 August 7 (TJD 11032) and 1998 September 16 (TJD 11072) are  $N_H = 7.7 \pm 0.45 \times 10^{22}$  and  $8.1 \pm 0.7 \times 10^{22}$  atoms  $\text{cm}^{-2}$ ,  $\Gamma = 1.42 \pm 0.07$  and  $1.6 \pm 0.25$ , with absorbed fluxes (2–10 keV) of  $1.7 \times 10^{-10}$  and  $0.98 \times 10^{-10}$  erg  $\text{cm}^{-2}$   $\text{s}^{-1}$ , respectively. These fluxes indicate a steady and long term decline in the brightness of 4U 1630-47 (Tomsick & Kaaret 1999). Using an assumed distance of 10 kpc the latter flux corresponds to a luminosity of  $1.2 \times 10^{34}$  erg  $\text{s}^{-1}$ . For a direct comparison with Parmar et al. (1997) the luminosity in September over the 2–2.4 keV range with an absorption of  $0.2 \times 10^{22}$  atoms  $\text{cm}^{-2}$  was  $6 \times 10^{34}$  erg  $\text{sec}^{-1}$ . This is much brighter than the quiescent levels found by Parmar et al. (1997).

We calculated power density spectra for each BeppoSAX observation for the source and background. Of the two observations only the August observation had significant ( $> 5\sigma$ ) excess power. At this time there was at least 50% rms variability (4U 1630-47 & background) over the 0.004–128 Hz range. Most of the excess is below 5 Hz. The background (7% of the source count rate) could contribute at most ( $3\sigma$  upper limit) 10% rms to the source variability. Therefore, 4U 1630-47 had at least 40% rms variability in the 0.004–128 Hz range. The combination of high rms variability, and a power law energy spectrum indicate that 4U 1630-47 entered the low state.

## 4. DISCUSSION

As compared to previous observations of 4U 1630-47, what is surprising about the 1998 outburst is the sheer variety of timing behavior. We can tentatively link some of the QPOs seen from 4U 1630-47. The large amplitude QPO seen on the early rise (A) is similar in behavior to the 0.1–10 Hz QPO on the early rise of XTE J1550-564 (Cui et al. 1999). In both cases hard X-ray flux as seen by BATSE is declining and the spectrum in the PCA is softening. The 3.7–0.2 Hz QPO seen late in the outburst (F) by Tomsick & Kaaret (1999) and a 0.15 Hz QPO later by Dieters et al. (1998b) would be the same but in reverse. Given the evolution of the spectrum (soft to hard), this is reasonable. Finally, the large amplitude QPO seen on the early rise of the 1999 mini(?)-outburst (McCollough et al. 1999), would also be the similar type of QPO. In all cases the shape and amplitude of the broad-band noise is similar. However, the harmonic content of the decline QPO and those in 1999 are different from those on the rise. The appearance of these large amplitude QPO with strong flat-topped noise can not depend solely on mass accretion rate as measured by count rate, since they do not reappear during the decline D. These QPOs could well only appear in a restricted range in the color-color diagram and therefore of spectral parameters. Unfortunately, we cannot link the QPO of A with those of B as would be suggested by the analogy with XTE J1550-564 which showed QPO changing continuously from 0.1 to 10 Hz.



The quasi-periodic dips of B and b appear only when 4U 1630-47 is in a fairly narrow range of count-rate, and hardness. Their increase and then decrease in depth and frequency as the count rate and color-color diagram position steadily changes in B, indicates that there is some optimum conditions for their occurrence. The pair of QPOs, one stable at 13.5 Hz, the other with a count rate/frequency dependence, are associated with the same conditions, since they reappear in the b observations which are B-like excursions from C or D where neither QPO are present.

The 1998 outburst of 4U 1630-47 was clearly very complex. According to the canonical model for black-hole transients, as a function of increasing accretion rate a source should pass through the states in this order: LS/IS/HS/VHS, and of course in reverse order as accretion rate decreases again towards quiescence. As a first approximation, we can infer accretion rate from the observed X-ray flux, although this approach has to be followed carefully. During the course of our observations, covering most of the rise and decline (A through E), there is always a mixture of a soft and hard component.

At the beginning of the outburst (A), at a relatively low accretion rate, the colors indicate that the source is rather hard, with the energy spectrum dominated by a power law component (see Fig 1d) i.e. the soft component is  $< 20\%$  of the flux. The power density spectrum is similar to that of an IS (Belloni et al. 1997b), although the break frequency of the broad band noise component is rather low, possibly connected to the fact that these observations are made early in the outburst, when the source was moving from a LS to an IS.

Rather rapidly, the source increased in flux and moved to observations of type B. There is a transition period as both the relative contribution of the soft flux increases and the dipping behavior becomes established. Through B the soft flux increases due to a combination of steepening in the power-law and an increase in the flux from the soft spectral component. But at no time does the soft component dominate the flux. The power density spectrum is extremely complex and not easy to interpret. The dipping behavior is unlike the absorption dip(s) reported during the 1996 outburst. Superficially the dipping behavior appears like that of GRS 1915+105 (Belloni et al. 1997b) and GRO 1655-40 (Remillard et al. 1999) for which the evidence is that the dips are due to a disk instability. However, note that another and different type of dips are present for GRS 1915+105 (Belloni et al. 2000). Alternatively, the dips of 4U 1630-47 may be more like dips and “flip-flops” seen in the VHS of GX 339-4 (Miyamoto et al. 1991). A detailed comparison between these various dipping behaviors is needed. In addition, there are 3 peaks in the power density spectrum: one from a stable QPO near 13.5 Hz and the other two from an intensity-dependent QPO. The difference in QPO behavior with count rate suggests that the two QPO have different origins. There are numerous examples of QPO in this range, but only those of GRO 1655-40 show a combination of stationary and moving QPO (Remillard et al. 1999). However, the energy spectrum of GRO 1655-40 at this time shows the soft component dominating (like VHS) and there were no dips. The combination of dips and QPO initially suggests that type B behavior is a VHS but unlike the canonical VHS the soft component does not dominate the flux, and it is not the highest flux regime. Overall these “shoulder” observations do not fit in a clear

way any of the canonical states and seem to be peculiar.

Next, the source jumps to C and in terms of the broad band noise into an obvious HS. The power-law shape, its slope and amplitude are a good match to high states in both 4U 1630-47 and other BHC. The QPO is so weak that it could well have escaped detection by previous instruments. They are similar to those seen from GRS 1915+105 in the “soft branch” (Chen et al. 1997). However, the spectrum indicates a strong power law component contributing  $\sim 60\%$  of the unabsorbed flux which is unlike a HS. The transitions in and out of C are both  $\leq 1$  day, and amongst the most rapid ever seen.

The exit from C into D is marked as a drop in count rate, softening of the disk (soft) component, and a lowering of the absorption. Initially the soft component contributes most of the flux (60–70%), but this contribution declines as the count rate drops. Also the power law hardens. The power density spectra (see Fig. 2D) are not unlike some observed in GX 339-4 in its VHS (Miyamoto et al. 1991 i.e. their Fig 4b). Since the fluxes are lower in D and follow a probable HS, we can exclude a VHS and it is natural to identify these observations with an IS, which is known to show characteristics very similar to those of the VHS (van der Klis 1995). The changes in the spectrum (HS-like toward LS-like) and color-color diagram support the identification with an IS.

At later times (E), the power density spectra are not very detailed due to the lower statistics, but are similar to the IS spectra reported by Belloni et al. (1997a) and Méndez & van der Klis (1997). The colors and spectra indicate that the soft component decreased in relative strength and softened further as the power law flattened. The source seems to be on its way, via the reappearance of strong QPO and strong broad band noise, to the LS (high rms, power law energy spectrum), which was reached by the time of the BeppoSAX observations (G) well below the detection threshold of the PCA but much brighter than the quiescent emission (Parmar et al. 1997).

On the rise, the spectral evolution, the QPOs and their frequency evolution are very similar to that of XTE J1550-564 (Cui et al. 1999). This may not be that surprising given that both these sources have been caught very early in their outburst. In the past the wealth of information found during the rise phases of the outburst have been missed. The changes in spectrum (soft to hard) on the decline are similar to that of many transients. However, the power density spectra are unusual. They are similar to that of Cir X-1 as it moves from the “upper banana” (similar to HS) through the “lower banana” into an extreme “island state” (similar to LS) (Oosterbroek et al. 1995). This serves as a warning that the spectral/timing properties discussed here and for other sources are not unique to BHCs.

This work supported by NASA/LTSA-NAG5-6021 (Dieters, van Paradijs, Kouveliotou & Lewin), NAG5-7483 (Dieters), NAG5-7484 (Cui) and by the Netherlands Organization for Scientific research (NWO) under grants 614-51-002 and Spinoza-08-0.

## REFERENCES

- Barret D., McClintock J.E., & Grindlay J.E., 1996, *ApJ*, 473, 963
- Belloni T., & Hasinger G., 1990, *A&A*, 227, L33
- Belloni T., Méndez M., King A.R., van der Klis M., & van Paradijs J., 1997a, *ApJ*, 479, L145
- Belloni T., van der Klis M., Lewin W.H.G., van Paradijs J., Dotani T., Mitsuda K., & Miyamoto S., 1997b, *A&A*, 322, 857
- Belloni T., Méndez M., van der Klis M., Hasinger G., Lewin W.H.G., & van Paradijs J., 1996, *ApJ*, 472, L107
- Belloni, T., Klein-Wolt, M., Méndez, M., van der Klis, M., & van Paradijs, J., 2000, *A&A* submitted
- Boella G., et al., 1997, *A&AS*, 122, 327
- Chen X., Swank J., & Taam R.E., 1997, *ApJ*, 477, L41
- Cui W., Zhang S.N., Focke W., & Swank J.H., 1997, *ApJ*, 484, 383
- Cui W., Zhang S.N., Chen W., & Morgan E.H., 1999, *ApJ*, 512, L43 (astro-ph/981208)
- Cui W., 1999, in *ASP Conf Series Vol. 161, High Energy Processes in Accreting Black Holes* eds. J. Poutanen & R. Svensson (San Francisco, ASP), 97 (astro-ph/9809408)
- Dieters S.W., Belloni T., Kuulkers E., Harmon A.B., & Woods P.M., 1998a, *IAU Circ.*, 6823
- Dieters S.W., Woods P., Kouveliotou C., & van Paradijs J., 1998b, *IAU Circ.*, 6962
- Gilfanov M., et al., 1994, in *NATO Series, Vol 450, The lives of Neutron Stars*, ed. Alpar et al. 351
- Hjellming R.M., et al., 1999, *ApJ*, 514, 383
- Jahoda K., Swank J.H., Giles A.B., Stark M.J., Strohmayer T., Zhang W., & Morgan E.H., 1996, in *Proc SPIE 2808, EUV, X-ray and Gamma-Ray Instrumentation for Astronomy VII*, ed D.H.W. Siegmund & M.A. Gummin, (Bellingham, SPIE), 59
- Jones C., Forman W., Tananbaum H., & Turner M.J.L, 1976, *ApJ*, 210, L9
- Kuulkers E., Parmar A.N., Kitamoto S., Cominsky L.R., & Sood R.K., 1997a, *MNRAS*, 291, 81
- Kuulkers E., van der Klis M., & Parmar A.N., 1997b, *ApJ*, 474 L47
- Kuulkers E., Wijnands R, Belloni T., Méndez M., van der Klis M., & van Paradijs J., 1998, *ApJ*, 494, 733

- Levine, A.M., Bradt, H., Cui, W., Jernigan, J.G., Morgan, E.H., Remillard, R., Shirey, R.E., & Smith, D.A., 1996, *ApJ*, 469, L33
- McCollough M.L., Harmon B.A., Dieters S.W., & Wijnands R., 1999, *IAU Circ.*, 7165
- Méndez M., & van der Klis M., 1997, *ApJ*, 479, 926
- Méndez M., Belloni T., & van der Klis M., 1998, *ApJ*, 499, L187
- Miyamoto S., Kimura K., Kitamoto S., Dotani T., & Ebisawa K., 1991, *ApJ*, 383, 784
- Oosterbroek T., van der Klis M., Kuulkers E., van Paradijs J., & Lewin W.H.G., 1995, *A&A*, 297, 141
- Oosterbroek T., Parmar A.N., Kuulkers E., Belloni T., van der Klis M., Frontera F., & Santangelo A., 1998, *A&A*, 340, 431
- Parmar A.N., Stella L., & White N.E., 1986, *ApJ*, 304, 664
- Parmar A.N., Williams O.R., Kuulkers E., Angellini L., & White N.E., 1997, *A&A*, 319, 855
- Priedhorsky W.C, 1986, *Ap&SS*, 126, 89
- Remillard R.A., Morgan E.H., McClintock J.E., Bailyn C.D., & Orosz J.A., 1999, *ApJ*, 522, 397
- Rutledge R.E., et al., 1999, *ApJS* 124, 265 (astro-ph/9807235)
- Tanaka Y., & Lewin W.H.G., 1995, in *X-ray Binaries*, ed W.H.G. Lewin, J. van Paradijs, & E.P.J. van den Heuvel, (Cambridge, Cambridge University Press), 126
- Tomsick J.A., Lapshov I, & Kaaret P., 1998, *ApJ*, 494, 747
- Tomsick J.A., & Kaaret P., 1999, *ApJ*, in press
- Van der Klis M., 1995, in *X-ray Binaries*, eds. W.H.G. Lewin, J. van Paradijs, and E.P.J. van den Heuvel, (Cambridge, Cambridge University Press), 252
- Woods P.M., Kouveliotou C., van Paradijs J., Hurley K., Kippen R.M., Finger M.H., Briggs M.S., Dieters S., & Fishman G.J., 1999, *ApJ*, 519, L142 (astro-ph/9903267)
- Zhang W., 1995, XTE PCA Internal Memo 5-23-95
- Zhang W., Jahoda K., Swank J.H., Morgan E.H., & Giles A.B., 1995, *ApJ*, 449, 930

Fig. 1.— The left-hand panels show the ASM and PCA light curves for the 1998 outburst. On the ASM light curve (top left panel) the times of all pointed observations are marked. The PCA count rates (lower left) are the background subtracted rates, over the full energy range ( $\sim 2\text{--}\sim 60\text{ keV}$ ), for PCU 0 only. The two right-hand panels show the hardness-intensity and color-color diagrams. The count rates and hardness ratio's are from PCU 0 only. The positions of the various timing/spectral behaviors are labeled, as in the text **A,B,C,D,E**. Label "b" indicates the reappearance of the dipping behavior of **B**. In the color-color diagram two sets of theoretical curves are shown: for a pure disk black-body and for a pure power law. Two different absorptions are shown:  $N_H = 8 \times 10^{22}$  (dotted) and  $N_H = 10 \times 10^{22}\text{ atoms cm}^{-2}$  (dot-dashed). As a reference, the rightmost points for the power-law model correspond to a photon index of 2.2 for the  $N_H = 8$  and 2.3 for  $N_H = 10$ . The other points steepen in steps of 0.1 and go until  $\gamma = 4.0$ . The disk black body points close to  $Y=1.0$  are  $kT=1.4$  ( $N_H = 8$ ) and  $kT=1.3$  ( $N_H = 10$ ).

Fig. 2.— Representative power density spectra in chronological order (top to bottom) through the 1998 outburst. Throughout the text the different types of timing behavior are referred to by their label within this figure i.e., A,B,C,D,E.

Fig. 3.— Light curve (Standard 1) over the  $2\text{--}60\text{ keV}$  range showing the dipping behavior in B. The observation was made on 1998 February 13 (TJD 50857).

Table 1. Broad band noise and QPO fit parameters.

	Count rate c/s/5PCU's	Noise fit parameters				QPO fit parameters		
		% rms 0.01-100 Hz	$\nu_{break}$	$\alpha < \nu_{break}$	$\alpha > \nu_{break}$	% rms	FWHM Hz	Frequency Hz
A	1426.34	$19.01^{0.56}_{0.77}$	$0.67 \pm 0.03$	0.0 Fixed	$1.44^{0.03}_{0.07}$	$17.03^{0.18}_{0.38}$	$0.2113^{0.006}_{0.015}$	$2.677^{0.0045}_{0.0054}$
						$7.93^{0.66}_{0.83}$	$0.95 \pm 0.013$	$3.33^{0.06}_{0.15}$
						$5.79^{0.41}_{0.48}$	$1.49^{0.19}_{0.22}$	$5.60 \pm 0.05$
B	4710.85	$2.09^{0.13}_{0.12}$	$2.26^{0.10}_{0.14}$	$0.51^{0.048}_{0.082}$	$1.78^{0.19}_{0.14}$	$2.876^{0.041}_{0.050}$	$1.072^{0.045}_{0.045}$	$4.953^{0.017}_{0.017}$
						$4.340^{0.032}_{0.070}$	$3.321^{0.065}_{0.075}$	$7.048^{0.030}_{0.033}$
						$2.035^{0.029}_{0.0485}$	$1.682^{0.060}_{0.100}$	$13.674^{0.022}_{0.018}$
						$2.119^{0.071}_{0.0905}$	$4.71^{0.85}_{0.50}$	$0.91^{0.18}_{0.10}$
C	5736.95	$1.63^{0.15}_{0.13}$		$1.13^{0.09}_{0.08}$		$2.29^{0.25}_{0.19}$	$6.9^{2.1}_{1.5}$	$8.16^{0.45}_{0.50}$
D	3724.48	$1.35^{0.35}_{0.22}$		$1.35^{0.27}_{0.20}$		$2.28^{0.27}_{0.22}$	$2.92^{0.46}_{0.42}$	$0.80^{0.20}_{0.28}$
						$1.15^{0.12}_{0.10}$	$5.26^{1.66}_{1.21}$	$10.54^{0.52}_{0.50}$
E	893.21	$1.42^{0.22}_{0.22}$	$1.28^{0.78}_{0.24}$	0.0 Fixed	$1.38^{1.915}_{0.28}$	$1.80^{0.15}_{0.15}$	$0.0539^{0.0178}_{0.0168}$	0.0 Fixed
						$2.11^{0.32}_{0.25}$	$4.8^{1.7}_{1.2}$	$10.59^{0.53}_{0.51}$

Note. — The broad band noise and QPO fit parameters of the 5 representative power density spectra shown in Fig. 2. A broken power law is used for A,B,E and a power law is used for C to model the broad band noise. Lorentzian peaks are used to model any QPO peaks and broader “bumps”. For A, the addition of a 0.34 FWHM bump at 0.55 Hz with 8.8% rms amplitude can also be added, but for only the first observation. For D two equivalent models were used: (top) a power law with a “bump” and a QPO, (bottom) a broken power law with a zero frequency Lorentzian and QPO. The “bump” and zero frequency Lorentzian can be considered extra components of the broad band noise. The errors are the  $1\sigma$  single parameter error i.e.; the parameter range within  $\Delta\chi^2 = 1.0$  of the best fit minimum.

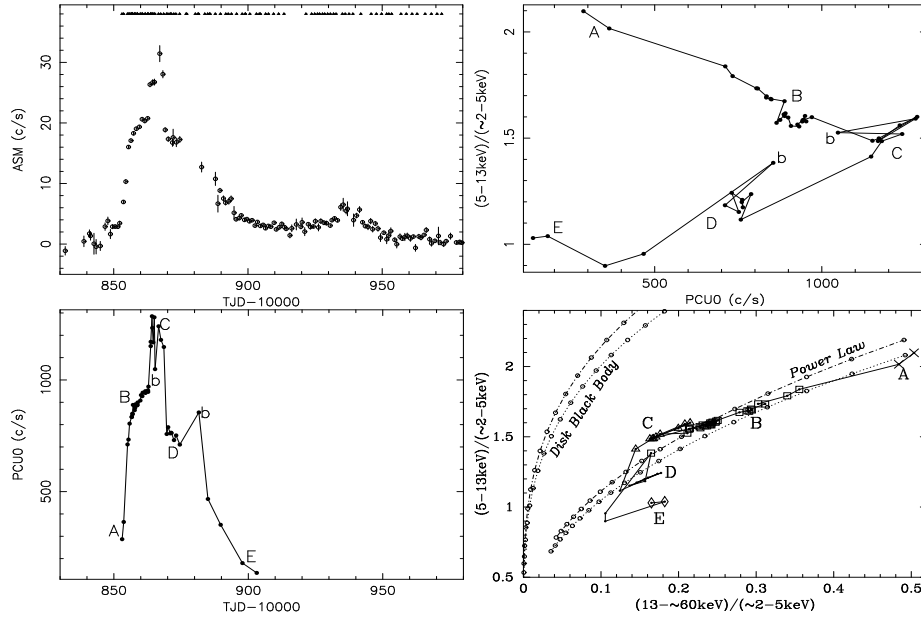


Figure 1

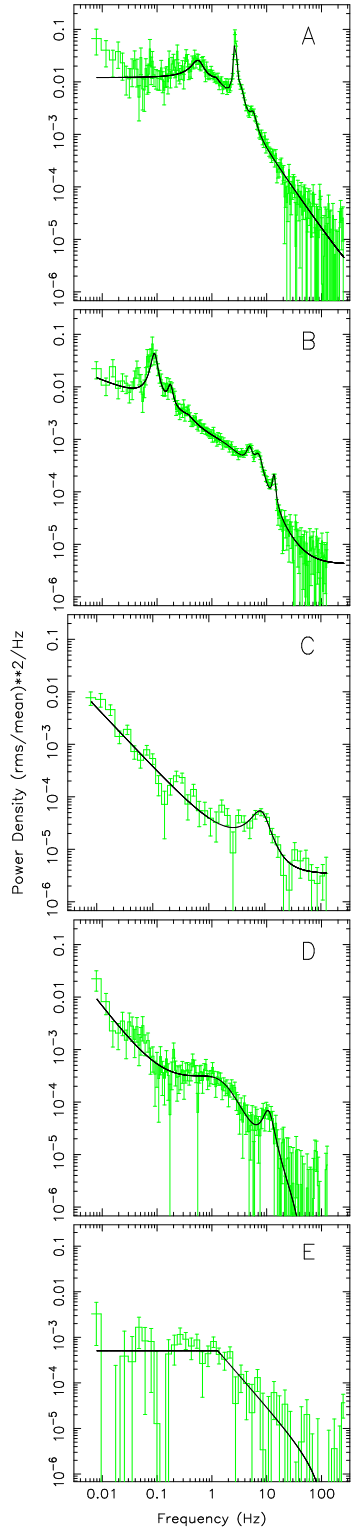


Figure 2



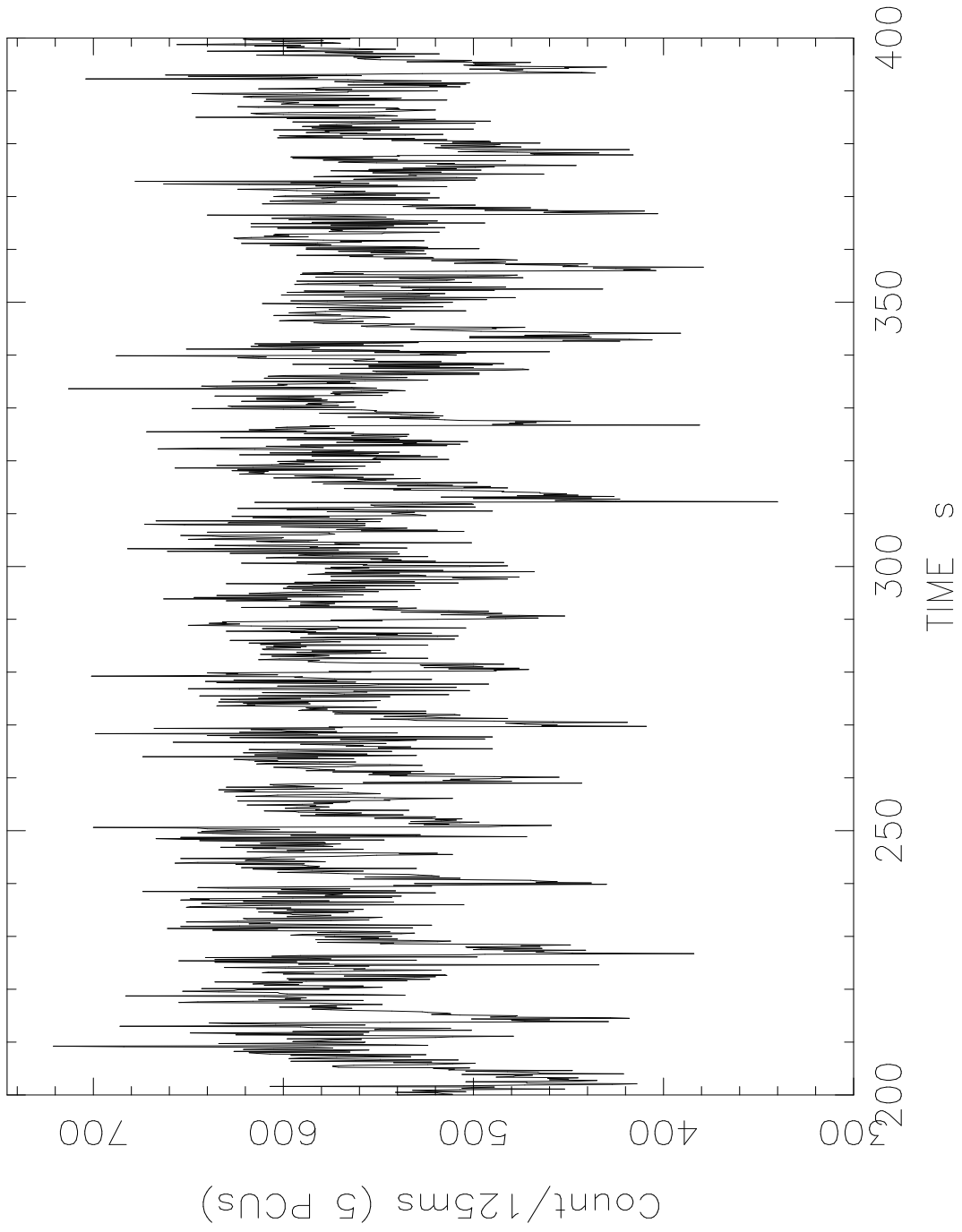


Figure 3